

REPORT DOCUMENTATION PAGE

Form Approved
OMB No. 0704-0188

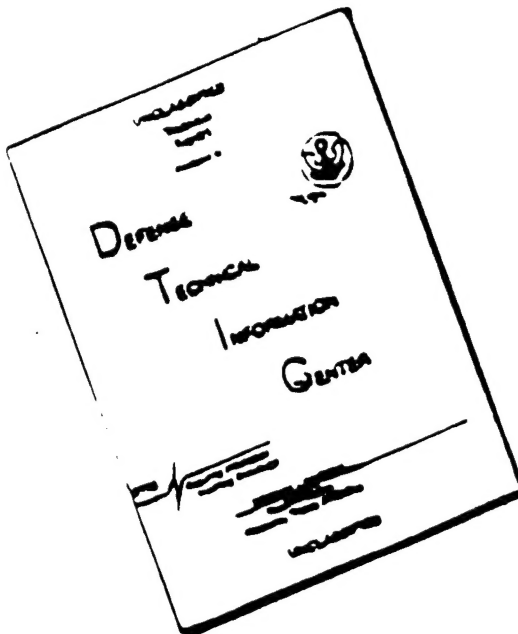
Public reporting burden for this collection of information is estimated to average 1 hour per response, including the time for reviewing instructions, searching existing data sources, gathering and maintaining the data needed, and completing and reviewing the collection of information. Send comments regarding this burden estimate or any other aspect of this collection of information, including suggestions for reducing this burden, to Washington Headquarters Services, Directorate for Information Operations and Reports, 1215 Jefferson Davis Highway, Suite 1204, Arlington, VA 22202-4302, and to the Office of Management and Budget: Paperwork Reduction Project (0704-0188), Washington, DC 20503.

1. AGENCY USE ONLY (Leave Blank)	2. REPORT DATE	3. REPORT TYPE AND DATES COVERED																					
	See Title Page	1 February 1987 to 31 January 1991																					
4. TITLE AND SUBTITLE			5. FUNDING NUMBERS																				
Use Title on Reprint One Copy of Each Submitted			N00014-87-C-0146 0R0A444C- 43051 43051S4																				
6. AUTHOR(S)			8. PERFORMING ORGANIZATION REPORT NUMBER																				
See Individual Articles																							
7. PERFORMING ORGANIZATION NAME(S) AND ADDRESS(ES)			9. SPONSORING/MONITORING AGENCY NAME(S) AND ADDRESS(ES)																				
Vanderbilt University Nashville TN 37332 (615-322-2786)			Office of Naval Research 800 North Quincy Street Arlington, VA 22217-5660																				
11. SUPPLEMENTARY NOTES			10. SPONSORING/MONITORING AGENCY REPORT NUMBER																				
Each Paper Summarized on first page. Journal articles submitted as contract reports. All work performed under Government contract.																							
12a. DISTRIBUTION/AVAILABILITY STATEMENT			12b. DISTRIBUTION CODE																				
Approved for public release; distribution unlimited.			<table border="1" style="width: 100%; border-collapse: collapse;"> <tr> <td colspan="2">Accession For</td> </tr> <tr> <td>NTIS</td> <td>CRA&I <input checked="" type="checkbox"/></td> </tr> <tr> <td>DTIC</td> <td>TAB <input type="checkbox"/></td> </tr> <tr> <td colspan="2">Unannounced <input type="checkbox"/></td> </tr> <tr> <td colspan="2">Justification _____</td> </tr> <tr> <td colspan="2">By _____</td> </tr> <tr> <td colspan="2">Distribution / _____</td> </tr> <tr> <td colspan="2">Availability Codes</td> </tr> <tr> <td>Dist</td> <td>Avail and / or Special</td> </tr> <tr> <td>A-1</td> <td></td> </tr> </table>	Accession For		NTIS	CRA&I <input checked="" type="checkbox"/>	DTIC	TAB <input type="checkbox"/>	Unannounced <input type="checkbox"/>		Justification _____		By _____		Distribution / _____		Availability Codes		Dist	Avail and / or Special	A-1	
Accession For																							
NTIS	CRA&I <input checked="" type="checkbox"/>																						
DTIC	TAB <input type="checkbox"/>																						
Unannounced <input type="checkbox"/>																							
Justification _____																							
By _____																							
Distribution / _____																							
Availability Codes																							
Dist	Avail and / or Special																						
A-1																							
13. ABSTRACT (Maximum 200 words)																							
See first page of Article																							
14. SUBJECT TERMS			15. NUMBER OF PAGES																				
Free Electron Lasers Medicine Biomedical Instrumentation Energy Cells			00																				
			16. PRICE CODE																				
17. SECURITY CLASSIFICATION OF REPORT		18. SECURITY CLASSIFICATION OF THIS PAGE	19. SECURITY CLASSIFICATION OF ABSTRACT																				
UNCLASSIFIED		UNCLASSIFIED	UNCLASSIFIED																				
			20. LIMITATION OF ABSTRACT																				
			UL																				

NSN 7540-01-280-5500

Standard Form 298 (Rev. 2-89)
Prescribed by ANSI Std Z39-18
298-102

DISCLAIMER NOTICE



**THIS DOCUMENT IS BEST
QUALITY AVAILABLE. THE COPY
FURNISHED TO DTIC CONTAINED
A SIGNIFICANT NUMBER OF
PAGES WHICH DO NOT
REPRODUCE LEGIBLY.**

The Role of Valence-Band Excitation in Laser Ablation of KCl

Richard F. Haglund, Jr., Kai Tang, Patrick H. Bunton^{*} and Ling-Jun Wang^{**}

Department of Physics and Astronomy
Vanderbilt University, Nashville, TN 37235

ABSTRACT

We present recent measurements of excited-atom and ion emission from KCl surfaces illuminated by vacuum-ultraviolet synchrotron radiation ($h\nu = 8\text{-}28 \text{ eV}$) and ultraviolet laser light ($h\nu = 4 \text{ eV}$). At low intensities characteristic of the synchrotron experiments, excited atoms are desorbed by simple valence-band excitation process involving the metallization of the KCl surface. At the higher intensities typical of laser desorption and ablation, we observe a strong decrease in K^* emission as a function of the number of laser shots, but an essentially constant yield of Cl^* . K^+ and Cl^- emission at high intensities show similar behavior. The energetics of these desorption phenomena can be treated in a bond-orbital model which shows that creation of a single valence hole is sufficient to excite an ion to an anti-bonding state.

1. INTRODUCTION AND MOTIVATION

The need to improve the laser damage resistance of optical materials, and the growing interest in the use of high-intensity lasers for processing electronic and photonic devices, are the primary drivers for fundamental studies of laser-surface interactions. Laser-induced surface¹ and bulk² damage in KCl have been studied for many years, perhaps because KCl is the simplest of all the wide-bandgap ionic solids from the standpoint of electronic structure. We have recently begun a systematic study of ultraviolet photon-stimulated desorption (PSD) of excited atoms and ions from the surface of KCl, which has led to new understanding of the mechanisms of desorption following both valence-band³ and core-level⁴ excitation. These experiments also illustrate the specific sensitivity of ion- and excited-atom desorption spectroscopy to details of the surface before and after particle emission.

In this paper, we briefly summarize the status of these experiments and propose a unified view for the mechanisms of PSD and laser-induced desorption (LID) and ablation of excited atoms in KCl, a view which probably applies generically to materials which have self-trapped excitons and/or permanent, mobile electronic defects, such as SiO_2 and the alkaline-earth halides. In the VUV experiments, the yield of desorbed excited atoms follows the excitonic optical response of these crystals at photon energies near the bulk band gap. Secondary electron measurements, taken simultaneously, implicate the formation of excess metal in PSD of excited alkalis, and suggest some clues to the time dependence of the M^* yields. At the higher intensities characteristic of LID and laser ablation, a common mechanism of desorption due to valence-hole creation, as well as charge exchange mediated by surface metallization, is at work.

The energetics governing desorption may be interpreted within the framework of a detailed mechanistic picture of laser-induced desorption and ablation, based on the bond-orbital model of electronic structure. In this model, ion motion is caused by localized deformation of the lattice and bond-breaking near the site where the photon is absorbed. Neutralization of the moving ion into an excited atomic state, on the other hand, is a manifestation of the local electronic structure near the desorption site, at least in the low-intensity limit. Both desorption and excitation may arise from the same mechanism. For example, desorption following valence-band excitation may be described as the decay of an excited quasi-molecular-state of the crystal; in KCl, the desorption of K^* could be initiated by relaxation of an excited F -center.

* Now at Department of Physics, Box 4608, Austin Peay State University, Clarksville, TN 37044

** Now at Department of Physics and Astronomy, University of Tennessee, Chattanooga, TN 37403

APPARATUS AND MEASUREMENTS

The following discussion of the role of valence-band excitations in laser-induced desorption from KCl is based on two distinct sets of measurements: photon-stimulated desorption (PSD) measurements using ultraviolet radiation, and laser-induced desorption (LID) using an excimer laser. The photon source for the PSD experiments was the Aladdin facility of the Synchrotron Radiation Center (SRC) at the University of Wisconsin. Bending-magnet radiation from the 800-MeV electron storage ring was dispersed by a Seya-Namioka (SN) normal-incidence monochromator and focused onto a sample at normal incidence. Useable photon flux is available in the approximate range of 8 eV to 28 eV. The light source for the LID measurements was an XeCl excimer laser operating at a wavelength of 308 nm, likewise incident along the surface normal.

Single-crystal targets of KCl, typically measuring 5x12 mm and cleaved from bulk material prepared by Harshaw were mounted on a micromanipulator in high or ultrahigh vacuum (UHV). In the UHV measurements, the target holder was equipped with a Varian button heater capable of heating targets to approximately 450° C. The target could be rotated about a vertical axis perpendicular to the plane of the incident photon beam.

Two generic measurement schemes were used in the experiments described in this paper. Fluorescence from desorbed excited alkali atoms was detected with an 0.3 meter monochromator and a photomultiplier (PMT) operated in pulse counting mode for the PSD measurements, and in pulse-height analysis mode, using a gated integrator, for the LID measurements. Amplified PMT pulses which exceeded the threshold of a discriminator were counted and stored in an Apple microcomputer. Secondary electrons were collected by a biased stainless-steel collector positioned close to the target; the current was monitored by a picoammeter connected to an analog-to-digital converter channel of a Hewlett-Packard 7090A plotter; these data were then likewise stored in the computer. All of the PSD experiments and most of the LID measurements were carried out in an ultra-high vacuum chamber with a base pressure generally in the range of $\sim 10^{-10}$ Torr.

In other LID experiments, the optical detection system shown in Fig. 1 was replaced by a quadrupole mass spectrometer which could be operated to collect either positive or negative ions. A mass scan was performed to ascertain that the peak corresponding to a particular mass was stable and well above background. Then an electronic gate was set to capture the peak signal after each laser shot. These peak height data were stored on-line in an IBM microcomputer for subsequent retrieval and analysis.

In the PSD experiments, single KCl crystals were cleaved in air and inserted immediately into the UHV chamber; they were typically under vacuum within an hour after cleaving. The UHV system was then baked at 200°C for several hours following insertion of the target; samples were then cleaned by heating a few hours at 300 to 400° C. Numerous studies, cited in Reference [4], have shown that this procedure yields a stable and reproducible surface. For the LID experiments, the samples were cleaved in air using the same precautions (use of rubber gloves, methanol cleaning of all cleaving and handling tools)

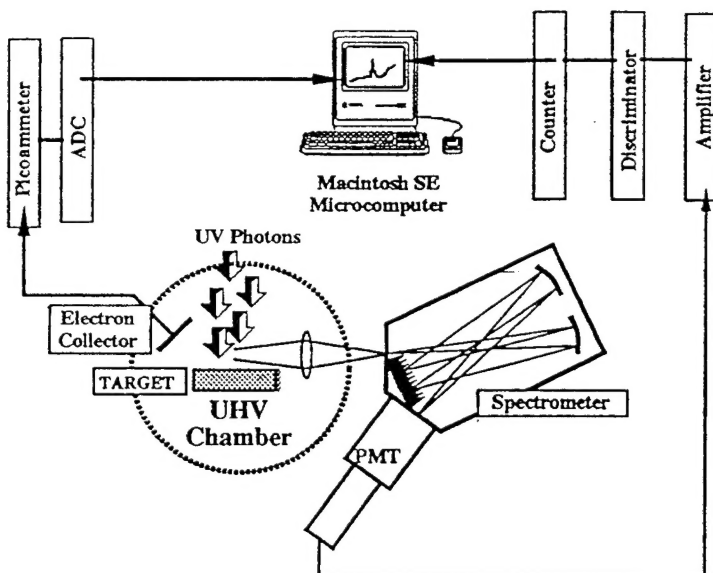


Figure 1. Schematic diagram of apparatus for simultaneous measurements of excited-atom yield and secondary-electron current in photon-stimulated desorption experiments.

which in preparing UHV samples. However, the samples were not baked, and indeed were not always in ultrahigh vacuum. We assume that the surface is well cleaned due to sputtering by the high-intensity laser pulses. Thus these laser desorption and ablation experiments must be viewed as having been carried out under reproducible conditions, but not necessarily on well-characterized surfaces.

3. PHOTON-STIMULATED DESORPTION IN THE VACUUM ULTRAVIOLET

Ultraviolet photon-stimulated desorption has been studied in the alkali halides for many years. Only recently, however, has it been demonstrated that PSD of excited atoms can be caused by valence-band, in contrast to core-level, excitation. Because these measurements have an important impact on our understanding of the mechanisms of laser-induced desorption, we summarize briefly the results of these recent experiments on both KCl and LiF. Details may be found in Reference [4].

Figure 2 shows an excitation function for desorbed excited potassium under photon irradiation of KCl near the surface exciton peak at 9.5 eV. The bulk bandgap of KCl is 8.4 eV. The monochromator flux was too low to search for structure in the desorption curve at lower energies. Shown for comparison in Figure 3 is the optical absorption spectrum of KCl measured by Eby, Teegarden and Dutton.⁵ Structure in the excitation function for desorbed K* corresponding to the valence exciton at approximately 9.5 eV is evidence that desorption due to valence excitation in KCl is occurring, and that excited-atom desorption may be related to identifiable electronic excitations of the surface.

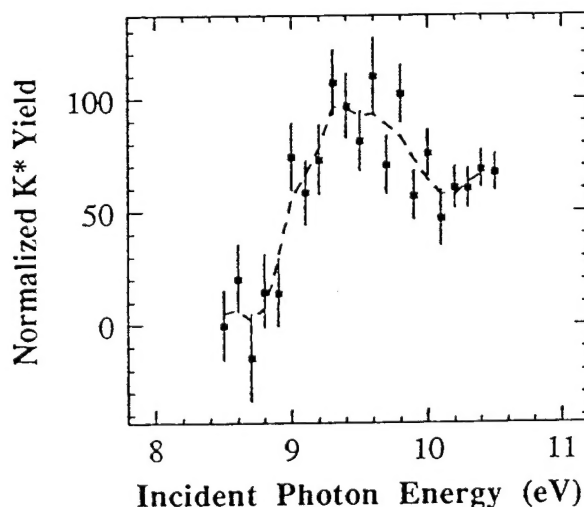


Figure 2. Excitation function for K* atoms desorbed from a KCl surface by VUV light with valence-band energies. From Reference [4].

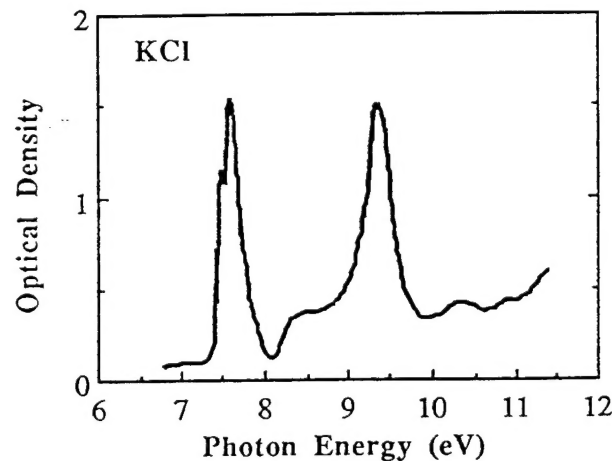


Figure 3. Optical absorption spectrum from KCl in the vacuum ultraviolet region. Figure is from Reference [5].

Studies of the variation in excited-atom and total electron yield, described in detail in Reference [4], clearly implicate the formation of excess metal on the surface in the desorption process. Those experimental results are consistent with the following picture: As a pristine spot on the surface is irradiated, metallization begins due to two separate processes. One is the loss of halogen because of the preferential ejection of ions from the halogen sublattice; the other is the creation of mobile defects (*e.g.*, F⁻ centers) in the near-surface bulk and their subsequent diffusion to the surface, where they neutralize the positive metal ions. The experimental evidence for this is primarily the rapid decrease in secondary electron yield from the high values which characterize the insulating surface as cleaved to the lower values (an order of magnitude or more for most of the alkali halides) characteristic of the alkali metal.⁶

This uncontrolled metallization can be stopped by annealing the sample at a temperature where the metal will evaporate thermally, leaving a stoichiometric surface. These thermally desorbing atoms constitute the bulk of the total desorption yield of the metal atoms, in the ground electronic state.⁷ The metallization also affects the yield of excited atoms, because as the metal agglomerates, its work function changes. When the metallic patches are small, the work function of the surface is rather large, and there are no metallic electrons which can be donated to fill the electronic state of a desorbing alkali ion. As metallization progresses, the work function decreases, and when the Fermi level is nearly resonant with the atomic excited state, neutralization of the ion into that excited state is probable. As the surface becomes more strongly metallized, the Fermi level of the metal patches rises *above* the first excited electronic state, and resonant charge exchange into the ground state becomes the dominant process. Thus, below the temperatures at which the metal evaporates, excited state desorption will first increase and then decrease as the Fermi level rises above the first excited state of potassium.

4. LASER-INDUCED DESORPTION AND ABLATION FROM KCl

The description of laser-induced particle emission is as problematical as the phenomenon itself is complex. In the following discussion, we shall refer to particle emission at low laser intensities as laser-induced desorption (LID); we mean to imply by this the absence of plasma and collective effects, and that the particle emission is, in this case, essentially a localized event resulting in the removal of an isolated atom or ion from an (at least hypothetically) identifiable surface site. By laser ablation we refer to the high-intensity limit, in which rapid damage to surface may involve collective effects and the generation of a plasma plume; in laser ablation, the characterization of the surface site is probably not possible.

We have carried out a series of experiments to study the change in the surface of KCl by monitoring the yields of excited atoms and ions from the surface, including K^* , Cl^* , K^+ and Cl^- . We have studied the change in K^* and Cl^* yields as a function of number of shots on the sample, and as a function of intensity. In addition, we have carried out simple measurements of the time dependence for the emission of positive and negative ions from the surface. These measurements are consistent with the PSD picture, but show in addition that laser-induced desorption (LID) proceeds through the same mechanism independent of the condition of the surface. Hence, LID from perfect lattice sites and defect sites appears to result from the same kind of valence-band excitation as observed in PSD, but with slightly different consequences because of the high density of local electronic excitation.

4.1 Laser-Induced Desorption of Excited Atoms

Optical spectra taken during laser ablation experiments generally show a relatively broad fluorescence background on which are superimposed atomic emission lines from excited atoms, radiating as they move away from the surface. In contrast to PSD experiments, we observe not only the first resonance line of the metallic atom, but lines originating in other excited states and the atomic emission lines of chlorine atoms and ions. Of particular interest is the appearance of excited-state emission whose parent states lie very near the ionization limits of the atoms in question; the mechanism for the creation of these highly excited states is not clear, although multiphoton excitation of ground-state atoms in the laser-produced plasma is probably the most likely possibility. Properties of the observed lines are shown in Table I.⁸

The calculated oscillator strengths shown in Table I are not always reflected in the relative spectral yields of the lines in question. This seems to be particularly true for the Cl^* states observed. We assume that this is indicative of highly nonequilibrium conditions which are likely to prevail both in the laser-produced plasma and at the surface. Also, the centroids of the lines as shown in the accompanying figures disagree slightly with those shown in the Table. Part of this discrepancy, typically 4 Å, is the result of calibration error in the spectrometer drive; the magnitude of the error was checked using a He-Ne laser at 6328 Å. In addition, since the excited atoms are emitted with non-zero velocity and since the spectrometer line-of-sight is not parallel to the surface plane, the lines will be Doppler shifted. This shift can, in principle, be calculated from a knowledge of the geometry of the desorption experiment.

Atomic Species	Wavelength (Å)	Atomic Transition	Upper Level (cm ⁻¹)	Lower Level (cm ⁻¹)	Oscillator Strength	Transition Rate (10 ⁸ s ⁻¹)
K	7676	4p → 4s	24,714	0	0.68	0.385
K	7699	4p → 4s	13,024	0	0.34	0.382
K	4045	5p → 4s	24,714	0	0.0091	0.0124
Cl	4105	$^3\text{p}^4\text{5P} \rightarrow ^3\text{p}^4\text{4S}$	96,309	71,954	$3.4 \cdot 10^{-4}$	0.002
Cl	4601	$^3\text{p}^4\text{5P} \rightarrow ^3\text{p}^4\text{4S}$	96,590	74,861	0.012	0.039
Cl	4624	$^3\text{p}^4\text{5P} \rightarrow ^3\text{p}^4\text{4S}$	96,482	74,861	0.0029	0.0045
Cl	4654	$^3\text{p}^4\text{5P} \rightarrow ^3\text{p}^4\text{4S}$	95,702	74,221	0.0016	0.0049
Cl	4661	$^3\text{p}^4\text{5P} \rightarrow ^3\text{p}^4\text{4S}$	96,309	74,861	0.0065	0.01

Figure 4 shows the spectrum of excited potassium atoms near the first resonance lines at 7668 Å, observed at laser intensities on the order of 1 GW·cm⁻². Each point on the spectrum represents a single laser shot; there are two hundred points in each spectral scan from 7600 to 7800 Å. Thus some 140 shots intervene between the upper spectrum and the lower. The decrease in the K* yield with absorbed photon dose is evident. This phenomenon is well known from PSD studies, in which progressive ultraviolet irradiation of the alkali halides results in a steady decrease of the excited-state atomic emission.⁹ This

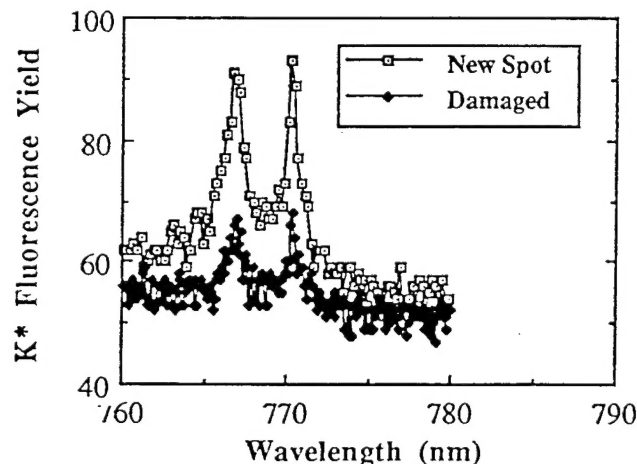


Figure 4. Spectrum of K* atoms desorbed from KCl at an intensity of 1 GW·cm⁻² on two successive scans, starting from a pristine spot on the surface. The atomic transition is 4p → 4s.

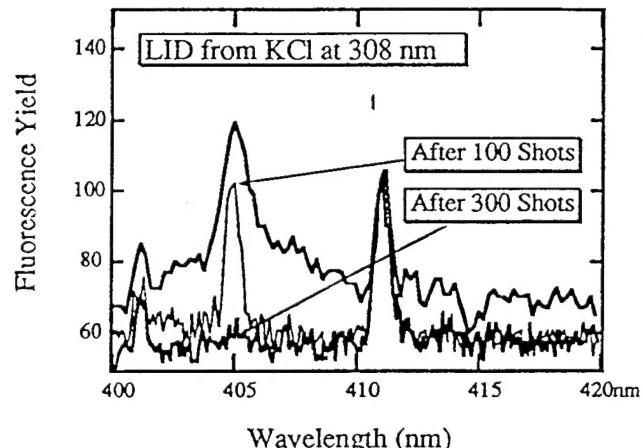


Figure 5. Optical spectrum of K* (405 nm) and Cl* (411 nm) atoms in the ablation plume from a KCl crystal surface at a laser intensity of order 1 GW·cm⁻², as a function of shot number.

behavior is consistent with a surface accumulation of excess metal leading to resonant ionization of desorbing K* atoms, thus reducing the total excited-state signal. Shown for comparison in Figure 5 are the relative yields of K* (from the 5p → 4s transition) and of Cl* emission originating from transitions in the ($^3\text{p}^4\text{5P} \rightarrow ^3\text{p}^4\text{4S}$) manifold. The K* emission in this state also decreases after a few hundred shots, consistent with the resonant ionization picture. The Cl* emission, on the other hand, is virtually constant in amplitude as a function of total absorbed dose, indicating that the Cl* production is not affected by surface conditions, such as metallization. Given the high excitation required to produce the parent states of these emission lines (nearly 12 eV, as shown in Table I), we suggest that multiphoton excitation of ground-state Cl in the laser-produced plasma is producing these signals. Accurate measurements of the Cl* yields as a function of intensity should reflect this difference in origin.

SPECTRA OF DESORBED ATOMS FROM KCL AT 308 NM

In these experiments, a region of the optical spectrum containing lines from K^* and/or Cl^* was scanned by the spectrometer, and the optical signal at each wavelength from a single laser pulse was counted. The excited K was only observed when there was a visible plasma. This could indicate that the surface is so rapidly metallized that one can only produce desorption following ablation of the metal, which should be strongly heated and vaporized at these intensities. Most notable is the contrast between the persistence of the Cl^* yield and the relatively rapid disappearance of any K^* signal.

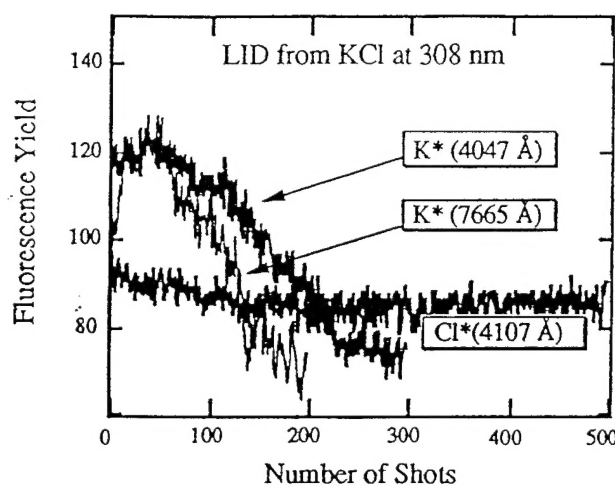


Figure 6. Spectrum of excited K atoms desorbed from KCl at an intensity of $1 \text{ GW} \cdot \text{cm}^{-2}$ starting from a pristine spot on the surface.

Figure 6 shows the yield of excited atoms desorbed from KCl at a laser wavelength of 308 nm and an intensity of about $4 \text{ GW} \cdot \text{cm}^{-2}$, as a function of the number of laser shots on a particular spot. The measurements begin, in each case, from a previously undamaged spot. The transitions identified in the Figure are the 7668 \AA line of K^* , the 4052 \AA line of K^* , and the 4112 \AA line of Cl^* . The variation in the behavior of the three species of excited atoms is : The K^* yields in both cases rise rapidly from the first laser shot, peak near the same value, and then drop off, but the $K^*(7668 \text{ \AA})$ yield goes to its background value after about 200 shots, where the $K^*(4052 \text{ \AA})$ yield does not decrease to background level for some 300 shots. The Cl^* yield, on the other hand, is essentially unchanged through the entire sequence. This behavior is consistent with the idea that excited K atoms are created in a different process than the excited Cl atoms.

If, indeed, resonant ionization of desorbing excited metal atoms is the mechanism, these data are consistent with the idea of progressive metallization of the surface with dose, since the Fermi level of the metal clusters would rise through the $4p \rightarrow 4s$ transition energy before the $5p \rightarrow 4s$, taking flux out of the former K^* channel prior to the latter.

4.3 Intensity Dependence of Positive and Negative Ion Yields

Yields of positive and negative ions were measured as a function of intensity using a quadrupole mass spectrometer in the geometry of Figure 1. In general, at laser intensities below $100 \text{ MW} \cdot \text{cm}^{-2}$, stable ion signals were measured which showed that ion yield increased with roughly the second power of intensity. This is consistent with valence-band excitation. However, above this intensity the ion signals rapidly became unstable, and showed an initial high yield followed by a rapid drop in intensity. This phenomenon was observed for both K^+ and Cl^- ions, as shown in Figures 7 and 8.

After the ion yields dropped to their minimum values and the visible plasma indicating desorption of excited atoms disappeared, it was observed that bright fluorescence from color centers was being excited by the laser beam. No other signs of damage to the surface - cratering or etching - were observable by eye. As soon as the laser beam was directed to a fresh spot on the surface, the strong ion signal was once again observed. This suggests that the disappearance of the Cl^- signal and the diminution of the K^+ signals are both tied to the creation of defects in the near-surface region of the bulk. The initial high yields in both ion species apparently comes from defect sites, while K^+ originates, at a low level, in the perfect sites. The Cl^- ions, on the other hand, are apparently only ablated from defect sites, and once the surface becomes stoichiometric, the negative ion signal disappears too. Cl neutral atoms, of course, continue to be produced, as shown above and in the neutral Cl laser-desorption measurements of Reference [1].

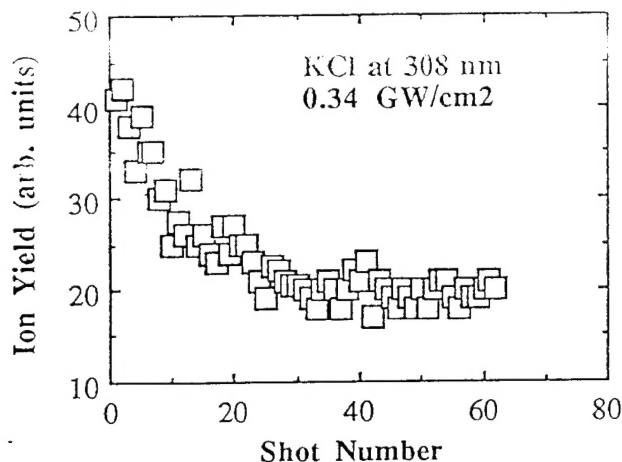


Figure 7. Intensity dependence of K^+ desorbed from KCl by an excimer laser (XeCl) at a wavelength of 308 nm. Intensity in the focal spot was 0.34 $\text{GW}\cdot\text{cm}^{-2}$.

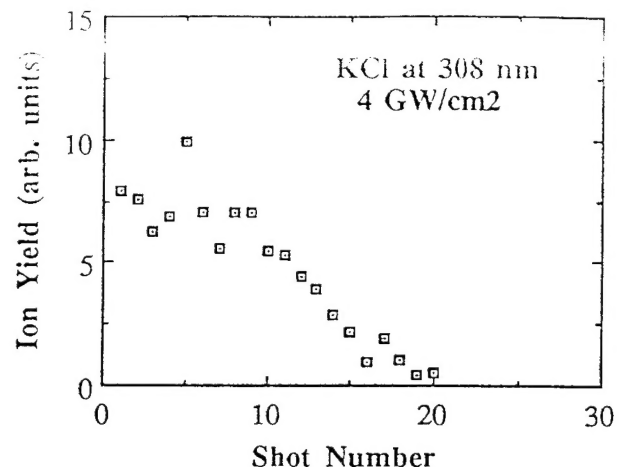


Figure 8. Intensity dependence of K^+ desorbed from KCl by an excimer laser (XeCl) at a wavelength of 308 nm. Intensity in the focal spot was about 4 $\text{GW}\cdot\text{cm}^{-2}$.

4.4 Time Dependence of Ion Yields

We have measured the time dependence of positive and negative ion yields from KCl by placing a biased stainless steel probe in the UHV chamber approximately 4 cm from the surface of the target and at an angle of 45° to the target normal. By switching the polarity of the probe from +67 V to -67 V, it was possible to collect both the positive and negative charges. For that voltage, the time of flight for a typical alkali ion is of order 4 μs and that for fast electrons is about 16 ns. Ion current was recorded on a synchronized single-shot basis by a 100 MHz transient waveform recorder interfaced to a microcomputer.

Figure 9 shows the transient signals of both positive and negative ions desorbing from the KCl crystal surface. The positive ion signal has an apparent decay time of some 25-30 μs , much longer than that measured for NaCl, and is initiated well after the negative ion fast signal has already begun to decay. The current of negative ions has both a fast and slow component. The slow component can be strongly suppressed by applying a magnetic field, and is thus assumed to consist primarily of slow electrons. The decay

time of the fast negative ion signal is much less than that of the K^+ signal, indicating that the Cl^- ion is desorbed by a different mechanism than the positive ions. This is consistent with earlier results from electron-stimulated desorption studies which show that neutral halogens are ejected from the surface before sodium atoms, and that the halogen is ejected in a non-thermal process on a time scale much less than 100

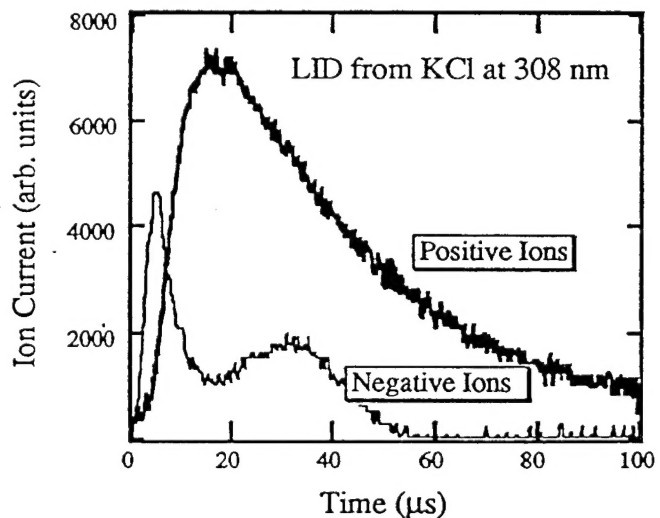
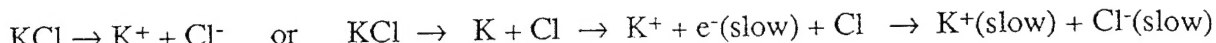


Figure 9. Time dependence of positive and negative ion signals following desorption from KCl by an excimer laser (XeCl) at a wavelength of 308 nm. Intensity in the focal spot was of order 1 $\text{GW}\cdot\text{cm}^{-2}$.

μs.³ The slow emission of electrons is particularly interesting, it may signal atoms desorbed out of the laser-produced plasma plume.

The differences in the behavior of the positive and negative ions suggests that there are mainly two processes involved: One is the direct desorption of the positive and negative ions, producing both the fast negative ion peak and the initial rise in the positive ion peaks. The second process proceeds through desorption of neutral atoms followed by ionization. These two processes are, schematically:



Since we do not yet have an accurate determination of how much of the slow negative-ion peak is actually electrons and how much is Cl^- , we can not yet rule out either of the two final states of the neutral-atom channel. Indeed, there is no reason to think that the late negative-ion peak might not include both components.

5. MECHANISM OF PHOTON-STIMULATED DESORPTION IN ALKALI HALIDES

Any proposed mechanism for LID or laser ablation of excited atoms or ions must answer two fundamental questions: (1) How is the absorbed photon energy localized to produce ion motion? and (2) What is the origin of the excited electronic state observed in the case of excited atoms or ions? We propose to discuss the first of these questions by referring to the bond-orbital model - a localized picture of electronic structure in solids within the framework of which bond-breaking has a particularly intuitive formulation. The question of the origin of the excited electronic state is particularly intriguing, and we show one example - applicable to KCl but not necessarily to alkali halides - of how such a state might be created by the decay of a highly localized excitonic state of the solid.

5.1 Energetics of Desorption Induced by Electron-Hole-Pair Creation

It is now generally accepted that laser induced desorption is related to the generation of a localized instability in the unperturbed crystal lattice.¹¹ Prior to the instant of desorption, the ion is in a band state with quantum numbers characteristic of the unperturbed lattice; following desorption, the ion (or atom) is a single-particle state with quantum numbers characteristic of its internal configuration, which may, of course, have been modified during the desorption process. The transition to the surface with a defect and a desorbing atom is the result of excitation from a bonding to an anti-bonding state, as described in the Menzel-Gomer-Redhead model.¹² This model, by itself, contains no specific information which would permit the computation of the details of the bonding and anti-bonding potentials; these details must be supplied from a model of the specific desorbing species and its surface environment.¹³

The initial event in this sequence is photon absorption and the creation of electron-hole pairs, which will depend on both the optical properties of the material and the laser wavelength. The absorbed photon, if it creates an electron-hole pair by valence-band excitation, breaks or weakens a bond. If the electron is in the conduction band - which would be typical of valence-band single-photon excitation or two-photon laser excitation in KCl - we are left with an electron in the conduction band and a much less mobile, usually self-trapped, hole. This electron can lose energy in one of two ways: by *delocalizing* in a band state, or by *self-trapping* through creation of a localized [metastable] lattice distortion. In the alkali halides, that metastable lattice distortion is called a self-trapped exciton. If the decay of that trapped exciton produces an atom on a repulsive potential energy surface, desorption will occur.

Thus the energetics of the desorption process are governed by the three parameters W (bandwidth), EST (the energy gained by self-trapping) and EDES (the energy available from "rolling down" the repulsive potential energy surface of the anti-bonding state). Desorption occurs if $W < EST$ and if $EDES > EST$.

One of the primary obstacles to making quantitative predictions about desorption lies in our inability to compute the energies W , E_{ST} and E_{DES} in a reliable and relatively simple way. We have calculated the initial effects of electron-hole pair formation following the bond-orbital theory of Harrison.¹⁴ In spirit, it is closely related to the bond-charge model of Phillips,¹⁵ although the details of the parametrization differ. In this model, the energy per bond in the perfect crystal is computed from the second and fourth moments of the density of states function using linear combinations of atomic orbitals, and is given by¹⁶

$$E_{\text{pair}} = -n \left[M_2 - \frac{M_4(\vartheta) - M_2^2}{4M_2} \right]^{1/2} + n \cdot V_0 + E_{\text{pro}}$$

where n is the coordination number; M_2 and $M_4(\vartheta)$ are, respectively, the second and fourth moments of the electronic density of states (EDOS); ϑ is the angle between neighboring bonds; V_0 is the repulsive screening potential; and E_{pro} represents the energy required to create the hybridized sp^3 bonds for the LCAO model of the solid. The fourth moment is a function of the bond angle ϑ , and will, in covalent solids, be influenced strongly by the dangling bonds and back-bonding required by surface reconstruction in those materials.¹⁷ In ionic materials, of course, we can expect much less dependence on the bond angle and more on the coordination number. The repulsive screening potential can be adjusted to fit the experimentally determined equilibrium inter-ionic spacing and the bulk modulus of the solid.

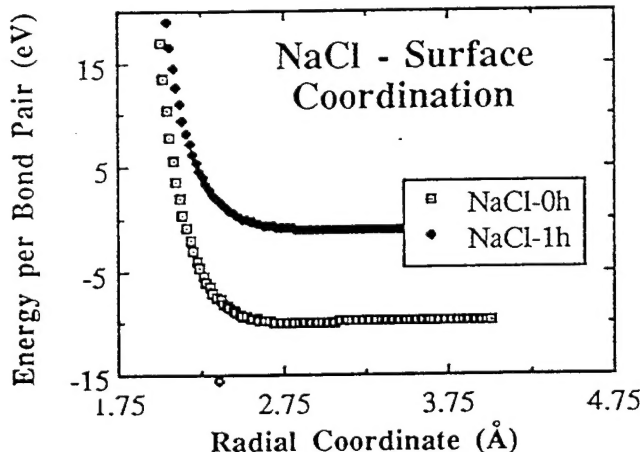


Figure 10. Bond-orbital calculation of the potential energy curves for a surface (five-fold) coordinated site in NaCl and for the same site with a one-hole excitation in a bond. The one-hole potential curve goes slightly negative at large radii.

We have used this expression for the energy per pair to model bond-breaking at a surface site in an ionic insulator. Because of their availability, we have used self-consistent Hartree-Fock matrix elements for NaCl taken from Reference [18] to calculate the moments M_2 and M_4 ; the same behavior can be expected from KCl. As an illustration of the technique, we show in Figure 10 the potential function that results when we begin with a five-fold (nearest-neighbor only) coordinated surface atom and create a hole in a single bond. One sees that the energy gained by creation of a single hole is already sufficient to put

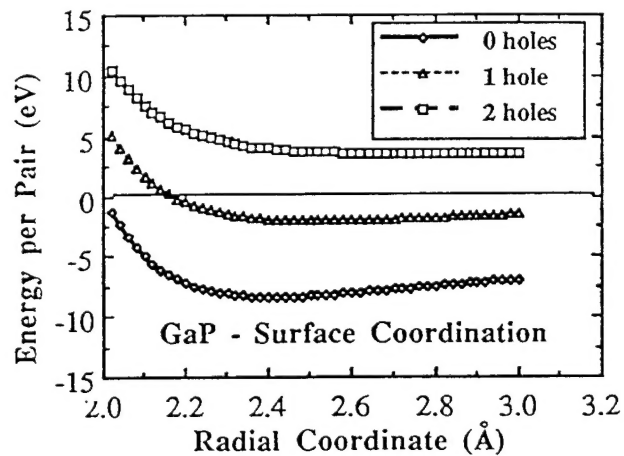


Figure 11. Bond-orbital calculation of the potential energy curves for a surface (three-fold) coordinated site in the compound semiconductor GaP and for the same site with one-hole and two-hole excitations. The one-hole potential curve is still characteristic of a weakly bound state.

and the energy of the $4p$ orbital is about 0.5 eV above the conduction band minimum. The potential energy of the $4p$ orbital is negative at large distances. This is probably a result of the fact that the bond-orbital model in this form assumes sp -hybridized bonds, whereas we know that the bonding orbitals in alkali halides are almost entirely of p character.

Thus, although it is qualitatively correct, this model still has some difficulties. Most notable is the fact that it does not yet properly account for the next-nearest neighbor interactions which are indispensable (and intractable!) in the alkali halides. Nevertheless, one sees by contrast with Figure 11 that the bond-orbital model at least shows a difference between the alkali halides - in which a single hole already puts the system on a repulsive energy surface - and the compound semiconductor GaP for which two holes are required to achieve the same end even though the binding energies are similar.

5.3 Source of the Excited Electronic State in Desorbing K Atoms

The origin of the electronic excitation which produces desorbing excited atoms is a separate but not unrelated question from the problem of ion motion we considered in Section 5.2. One possibility is that an excited F -center is the source of the excited atom desorption following valence excitation. Certainly valence excitation can form F -centers. It is conceivable that some of them may be excited, perhaps from scattering of secondary electrons, fluorescence, or, in the case of laser-induced desorption, by the high local density of electronic excitation. The strong coupling of an excited F -center to the lattice could both initiate ion motion and simultaneously provide the electron needed for neutralization of a departing ion. Such a mechanism would explain the observed decrease of the excited atom yield as a function of temperature in PSD measurements, since the lifetime of the excited F -center would decrease with increasing temperature. Alkali desorption (without reference to the electronic state of the atom) has been observed from RbBr containing F -centers during irradiation with F -band light.¹⁸

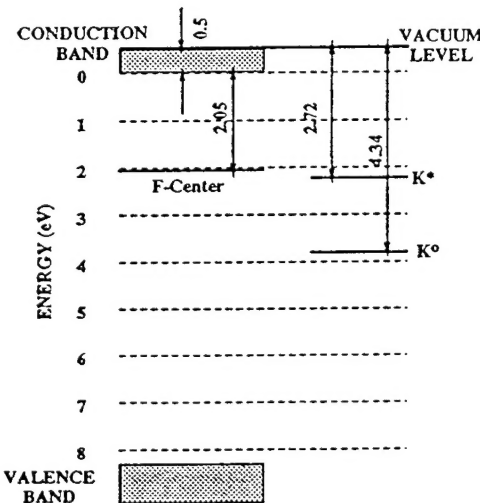


Figure 12. Energies of the $4p$ electronic state in the K atom and the relevant F -center energies in KCl. All energies are given in eV.

A simple consideration of the energetics will show that an excited F -center in KCl has about the right energy to neutralize a potassium ion into the first excited state of the neutral. Figure 12 shows an approximate band diagram for KCl including an F -center. Notice that the ground state F -center is almost resonant with an excited neutral alkali atom, so the excited state will clearly have sufficient energy to do so. The thermal ionization energy of the F -center¹⁹ was used to position the F -center below the conduction band. The ionization limit of the atom was made coincident with the vacuum level of KCl. These methods are approximate, since both the lattice distortion and the surface of itself will alter the band structure; indeed, the lattice relaxation - an essential feature in the dynamics of desorption - will almost certainly modify the relative energies of the various levels shown here.

Localized vibrational excitations of the charged lattice could also produce electronic excitation in a desorbing ground-state atom via electric dipole interactions. Calculations by Bickham and Sievers²⁰ show that excitation of a crystal with an anharmonic lattice potential can lead to the formation of localized vibrational modes of a solid. The energy required is typically that required for creation of an excited F -center. However, in the alkali halides, these modes are only formed for the two-dimensional lattice - consistent with the idea that this might be a purely surface phenomenon. That, of course, would fit the case either of PSD or laser desorption/ablation.

6. CONCLUSIONS

We have observed desorption and ablation of excited atoms and ions from the surface of KCl as a function both of dose and, in the case of ions, as a function of time following the arrival of the laser pulse. These experiments demonstrate the sensitivity of the excited-atom yields to the conditions of the surface, even at intensities characteristic of laser ablation; moreover, the excited atoms show evidence for a different dynamical origin than the ions, thus making them interesting objects of study.

Experimental results for laser-induced desorption and ablation are consistent with the low-intensity results of valence-band-induced desorption by synchrotron radiation. However, at high powers, there is evidence for desorption not only from perfect lattice sites but from defects created by the laser radiation. The final states of the desorbing atoms and ions appear to be strongly influenced by the metallization of the surface - a metallization arising from the preferential ejection of atoms and ions from the halogen sublattice of KCl. The defect sites which play a prominent role in the or shot-number dependence of the ion and excited atom yields at high intensities are energetically more susceptible to desorption than perfect lattice sites. Therefore, even though multiphoton excitation may be required initially to create the lattice defects, desorption can occur even for sub-bandgap photon energies characteristic of lasers because the electronic structure of the defects places them closer to the conduction band than the bulk bandgap energy.

The origin of the excited electronic state observed in desorbing atoms remains something of a mystery. While it is clear that the metallization of the surface plays a role in the initial creation of this state and in its temporal evolution with absorbed photon dose, we presently have no knowledge of the temporal evolution of either the ground-state or the excited state yields following irradiation by a laser pulse.

7. ACKNOWLEDGEMENTS

We are grateful to: the staff of the Synchrotron Radiation Center (SRC) for their expert handling of the Aladdin storage ring; Dr. Winston Chen of the Oak Ridge National Laboratory for the use of his laboratory in some of the laser ablation measurements; Mario Affatigato for his help with the ion ablation experiments; Dengfa Liu for assisting in the synchrotron radiation experiments; and Dr. Russell Dreyfus for illuminating discussions. This research was sponsored in part by the University Research Initiative of the Air Force Office of Scientific Research, by the SURA/ORAU/ORNL Summer Cooperative Program, and by the Medical Free-Electron Laser program managed by the Office of Naval Research for the Strategic Defense Initiative Organization. The SRC is supported by the National Science Foundation. Patrick H. Bunton was supported by a National Aeronautics and Space Agency training grant.

8. REFERENCES

1. A. Schmid, P. Bräunlich and P. K. Rol, "Multiphoton-induced directional emission of halogen atoms from alkali halides," Phys. Rev. Lett. 35 (1975) 1382.
2. Reviewed in S. C. Jones, P. Braunlich, R. T. Casper, X.-A. Shen and P. Kelly, "Recent progress on laser-induced modifications and intrinsic bulk damage of wide-gap optical materials," Opt. Eng. 28 (1989) 1039-1068.
3. P. H. Bunton, R. F. Haglund, Jr., D. Liu and N. H. Tolk, "Photon-stimulated desorption of excited alkali atoms following valence-band excitation of alkali halides," to be submitted to Phys. Rev. B.
4. P. H. Bunton, R. F. Haglund, Jr., D. Liu and N. H. Tolk, "Photon-stimulated desorption of excited alkali atoms from alkali halides following core level excitation," in press, Surf. Sci.

5. J. E. Eby, K. J. Teegarden, and D. B. Dutton, "Ultraviolet Absorption of Alkali Halides," Phys. Rev. **116**, 1099 (1959).

6. Secondary electron yields are tabulated with references in the *CRC Handbook of Chemistry and Physics*, R. C. Weast, ed., (Boca Raton, Florida: CRC Press, Inc., 1988), p. E-376.

7. N. G. Stoffel, Riedel, E. Colavita, G. Margaritondo, R. F. Haglund, E. Taglauer and N. H. Tolk, "Photon-stimulated desorption of neutral sodium from alkali halides observed by laser-induced fluorescence," Phys. Rev. B **32** (1985) 6805.

8. W. L. Wiese, M. W. Smith and B. M. Miles, *Atomic Transition Probabilities II: Sodium through Calcium*, NSRDS-NBS **22** (1965).

9. R. F. Haglund, Jr., M. H. Mendenhall, N. H. Tolk, G. Betz and W. Husinsky, "Surface and Near-Surface Radiation Effects in Photon-Stimulated Desorption," Nucl. Instrum. Meth. in Phys. Res. **B32** (1988) 321.

10. H. Overeijnder, R. R. Tol and A. E. DeVries, "Delay times in the sputtering of atoms from alkali crystals during low-energy electron bombardment," Surf. Sci. **90** (1979) 265.

11. K. Tanimura and N. Itoh, "Generation of Lattice Defects by Exciton Interaction in RbI: Lattice Instability under Dense Electronic Excitation," Phys. Rev. Lett. **60** (1988) 2753-2756.

12. D. Menzel and R. Gomer, "Desorption from metal surfaces by low-energy electrons," J. Chem. Phys. **41** (1964) 3311. P. A. Redhead, "Interaction of slow electrons with chemisorbed oxygen," Can. J. Phys. **42** (1964) 886.

13. Y. Nakai, K. Hattori, A. Okano, N. Itoh and R. F. Haglund, Jr., "Non-Thermal Laser Sputtering from Solid Surfaces," Nucl. Instrum. Methods in Phys. Res. B, to be published (1991).

14. W. A. Harrison, *Electronic Structure and the Properties of Solids* (New York: Dover, 1989).

15. J. C. Phillips, *Bonds and Bands in Semiconductors* (New York: Academic Press, 1973)

16. W. A. Harrison, "Interatomic interactions in covalent and ionic solids," *Physical Review B* **41** (1990) 6008-6019.

17. R. F. Haglund, Jr., K. Hattori and N. Itoh, "Bond-Orbital Model of Two-Hole Laser-Induced Desorption from Semiconductors," to be published.

18. H. Kanzaki and T. Mori, "Photon-stimulated desorption of neutrals from silver and alkali halides," Phys. Rev. B **29**, 3573 (1984).

19. N. Itoh, A. M. Stoneham, and A. H. Harker, "A theoretical study of desorption induced by electronic transitions in alkali halides," Surf. Sci. **217** (1989) 573; J. J. Markham, *F - Centers in Alkali Halides* (Academic Press, NY, 1966), p. 123.

20. S. R. Bickham and A. J. Sievers, "Intrinsic localized modes in a monatomic lattice with weakly anharmonic nearest neighbor force constants," submitted to Phys. Rev. B. We thank Professor Sievers for sharing this work with us prior to publication.